nerly named talktriplite, from Hållsjöberget
Geol. 2 (1956) 149–153.
ıltiger Wagnerit aus dem Val Ambra (Tessin,
1) (1984) 109–110.
ı Skřinářov, central Czechoslovakia. Neues
542.
Bayerischer Wald). Neues Jahrb. Mineral.
n Modum, Norway: Addendum. Lithos 12
Wagnerit, Althausit und Holtedahlit (das
schr. Mineral. 58 (Beiheft 1) (1980) 107–108.
a new magnesium phosphate from Modum,
ructure of ε-Mg_2PO_4OH, a synthetic high-
177 (1986) 1–13.
ew mineral from Modum, Norway. Lithos 8
cture of althausite, $Mg_4(PO_4)_2(OH,O)$ (F,□).
ıcture of heneuite, $CaMg_5(CO_3)(PO_4)_3(OH)$.
), 351–359.
E., Taylor, R. B.: Mineralogy and geology of
Mountain, Front Range, Colorado. U.S. Geol.
e from Czechoslovakia (in Slovak). Acta Mus.
kého Musea v Brné, Vědy Přírodní] 50 (1965)
n, W. T.: Coherent X-ray scattering for the
ule. J. Chem. Phys. 42 (1965) 3175–3187.
ıidite and its relation to the structures of other
p. Z. Kristallogr. 131 (1970) 1–20.
ZY PULVERIX, a computer program, for
ion powder patterns. J. Appl. Crystallogr. 10

Zeitschrift für Kristallographie 177, 27–38 (1986)
© by R. Oldenbourg Verlag, München 1986

Structural change of orthorhombic-*I* tridymite with temperature: A study based on second-order thermal-vibrational parameters

Kuniaki Kihara, Takeo Matsumoto and Moritaka Imamura*

Department of Earth Sciences, Faculty of Science, Kanazawa University, 1–1 Marunouchi, 920 Kanazawa, Japan

Received: April 7, 1986; in revised form July 6, 1986

Tridymite / Structure transition / Disorder

Abstract. X-ray studies of orthorhombic-*I* tridymite, especially focussed on atomic mean-square displacements (m.s.d.'s) at 443, 493, 573, 653 and 693 K respectively, were carried out on the basis of the usual second-order refinement of the Dollase model.

The m.s.d.'s for O are highly anisotropic, and large in the planes perpendicular to Si–Si axes. Plots of temperature vs. m.s.d.'s point to a disorder of O atoms in the orthorhombic-*I* form. The transition, from the orthorhombic-*I* to the hexagonal high form or vice versa, is an example of a displacive structure transition from a disordered structure to another disordered one. When temperature falls from 693 K, any two SiO_4 tetrahedra joined by O on the two-fold axes parallel to **a** move away from the hexagonal positions, rotating progressively around the two-fold axes, and then symmetry is lowered to orthorhombic. The pair-wise rotations are accompanied by anisotropic changes of the thermal ellipsoids for two kinds of O atoms forming the basal planes of silica tetrahedra, nearly normal to **c**; the thermal ellipsoids are distorted to elliptical shapes in the sections perpendicular to Si–Si axes when temperature falls. On the other hand, the thermal ellipsoid for the apical O atom is approximately circular in that section.

* *Present address:* Seien Joshi Gakuen High School, Sato-cho 343, Hamamatsu 430, Japan.

Introduction

Tridymite is a unique mineral, which shows successive structure transitions at atmospheric pressure. Monoclinic tridymite, from silica brick, at room temperature shows successively three transformations with increasing temperature: monoclinic (abbreviated as *M*), orthorhombic-*II* (*O*−*II*), orthorhombic-*I* (*O*−*I*) corresponding to the 'orthorhombic high' form of Dollase (1967) and hexagonal (*H*) (Kihara, 1977 and 1978). (*O*−*I* and *O*−*II* respectively correspond to *OC* and *OP* in Nukui et al., 1978.)

The conventional least-squares refinements of *O*−*II* at 428 K (Kihara, 1977), *O*−*I* at 493 K (Dollase, 1967) and the Gibbs model of *H* at 733 K (Kihara, 1978) showed unusually large and anisotropic thermal parameters for O. The thermal ellipsoids of O in *H* are oblate-spheroidal exactly for O1 and approximately for O2, with the smallest m.s.d. parallel to the directions joining two Si atoms bonded to O. In *O*−*I*, the spheroids are slightly distorted to elliptical (not circular) shapes in the planes nearly perpendicular to the Si−Si lines. Those in *O*−*II* are prolate-spheroidal with the largest axes perpendicular to the Si−Si lines.

The O thermal vibrations in the structure of *H* were more successfully refined for a 'split-atom model', i.e., a model of multimodal density distribution of O, where the atoms are statistically distributed over six sets of positions on circles, with radii about 0.4 Å, perpendicular to the Si−Si axes (Kihara, 1978). This split-atom model was also derived by a geometrical method using rigid SiO_4 tetrahedra (Kihara, 1980). Schneider et al. (1979) have independently proposed the same model.

The transformations between *M* and *O*−*II* and between *O*−*II* and *O*−*I* show a clear discontinuity in the cell dimensions and X-ray intensities, but that between *O*−*I* and *H* is continuous (Kihara, 1978). A detailed structural study of these transformations has not yet been reported. In the present study, the Dollase model of *O*−*I* in the usual second-order expansion was refined for five sets of X-ray structure factors at 443, 493, 573, 653 and 693 K, because the structure of *O*−*I* has been so far studied only by Dollase (1967) using the Steinbach tridymite at 493 K. Detailed studies of the remarkable thermal-vibrational parameters are expected to be useful for further understanding of the transformations in tridymite. Special attention was thus given to the thermal-vibrational parameters as function of temperature. All the computations were carried out on a microcomputer.

Experimental

A platy specimen (A # 3) with the largest dimension of 0.14 mm was picked up from the surface of refractory silica brick, which was previously used by Kihara (1977 and 1978). The sample from this silica brick is very pure

Table 1. Cell dimensions of tridymite

Temperature	*a*(Å)
443 K	8.730(
493 K	8.756(
573 K	8.764(
653 K	8.743(
693 K [a]	8.742(

[a] Measured as orthorhombic cells.
E.s.d.'s are in parentheses.

with only small amounts of Al
Na were detected, respectively
heating experiments, this specim
using a microscope and taking
electric furnace with a diamet
specimen. The X-ray intensities
in the range of θ from 3 to 30°
at 443, 493, 573, 653 and 69
diffractometer PW 1100, using
a thyristor regulator and a ther
fluctuation to be within 1 K
were converted into amplitudes
standard deviations of $|F_o|$'s
statistics alone. The cell constan
mined, using the least-squares n
ured on the diffractometer (Tab
on the basis of the orthorhomb

Refinements

There are four symmetry-inde
Dollase model of *O*−*I*. Si and O
while O1 and O2 are at the s
3/4), respectively, on two-fold ax
order expansion involves 28
20 coefficients for anisotropic
factor and an isotropic extinct
cell origin is shifted (1/4)**c** from
Tables for X-ray Crystallograph

The refinements converged
comparison, the refinements b
out for the structure factor dat

h shows successive structure transitions
ic tridymite, from silica brick, at room
hree transformations with increasing
ated as M), orthorhombic-II ($O-II$),
ding to the 'orthorhombic high' form
H) (Kihara, 1977 and 1978). ($O-I$ and
C and OP in Nukui et al., 1978.)
refinements of $O-II$ at 428 K (Kihara,
57) and the Gibbs model of H at 733 K
rge and anisotropic thermal parameters
in H are oblate-spheroidal exactly for
vith the smallest m.s.d. parallel to the
onded to O. In $O-I$, the spheroids are
t circular) shapes in the planes nearly
hose in $O-II$ are prolate-spheroidal with
he Si – Si lines.
e structure of H were more successfully
, a model of multimodal density distribu-
statistically distributed over six sets of
bout 0.4 Å, perpendicular to the Si – Si
-atom model was also derived by a
O_4 tetrahedra (Kihara, 1980). Schneider
roposed the same model.
M and $O-II$ and between $O-II$ and
the cell dimensions and X-ray intensities,
continuous (Kihara, 1978). A detailed
mations has not yet been reported. In
odel of $O-I$ in the usual second-order
s of X-ray structure factors at 443, 493,
tructure of $O-I$ has been so far studied
Steinbach tridymite at 493 K. Detailed
-vibrational parameters are expected to
ng of the transformations in tridymite.
to the thermal-vibrational parameters
he computations were carried out on a

largest dimension of 0.14 mm was picked
silica brick, which was previously used
ample from this silica brick is very pure

Table 1. Cell dimensions of tridymite at five different temperatures.

Temperature	a(Å)	b(Å)	c(Å)
443 K	8.730(11)	5.000(6)	8.201(6)
493 K	8.756(8)	5.024(3)	8.213(4)
573 K	8.764(14)	5.039(6)	8.235(7)
653 K	8.743(7)	5.046(4)	8.254(5)
693 K [a]	8.742(8)	5.047(4)	8.262(5)

[a] Measured as orthorhombic cells.
E.s.d.'s are in parentheses.

with only small amounts of Al and Na: about 50 and 140 ppm of Al and Na were detected, respectively, in electron probe microanalysis. Before heating experiments, this specimen was checked to be free from twinning by using a microscope and taking X-ray diffraction photographs. A spherical electric furnace with a diameter of about 10 mm was used to heat the specimen. The X-ray intensities of 322 symmetry-independent reflections, in the range of θ from 3 to 30°, were measured with the $\theta/2\theta$ scan mode at 443, 493, 573, 653 and 693 K, respectively, on a Philips four-circle diffractometer PW 1100, using monochromated MoK_α radiation. A set of a thyristor regulator and a thermocouple was used to control temperature fluctuation to be within 1 K during the measurements. The intensities were converted into amplitudes after Lp and absorption corrections. The standard deviations of $|F_o|$'s were estimated on the basis of counting statistics alone. The cell constants at five different temperatures were determined, using the least-squares method for 15 centroids of reflections measured on the diffractometer (Table 1). Those of H at 693 K were calculated on the basis of the orthorhombic cell.

Refinements

There are four symmetry-independent atoms, Si, O1,O2 and O3 in the Dollase model of $O-I$. Si and O3 are at the general positions, $8c$, of $C222_1$, while O1 and O2 are at the special positions $4a$ $(x,0,1/2)$ and $4b$ $(0,y,3/4)$, respectively, on two-fold axes. Thus the Dollase structure in the second-order expansion involves 28 adjustable parameters; 8 coordinates and 20 coefficients for anisotropic temperature factors, in addition to a scale factor and an isotropic extinction factor. It should be noted that the unit cell origin is shifted (1/4)**c** from that adopted for $C222_1$ in the *International Tables for X-ray Crystallography*, vol. I (1952).

The refinements converged at the parameters shown in Table 2: for comparison, the refinements based on the same model were also carried out for the structure factor data measured at 733 K by Kihara (1978). The

Table 2. Atomic parameters at 443, 493, 573, 653, 693 and 733 K: Refinements based on Dollase's model.

		443 K [a]	493 K [a]	573 K [a]	653 K [a]	693 K [a]	733 K [b]
Si	x	0.1685(4)	0.1681(2)	0.1682(3)	0.1686(4)	0.1673(3)	0.1668(3)
	y	0.5512(8)	0.5470(4)	0.5352(5)	0.5222(6)	0.5099(7)	0.4914(20)
	z	0.4380(5)	0.4379(3)	0.4380(4)	0.4382(4)	0.4378(3)	0.4377(3)
	$b11$	0.0076(4)	0.0095(3)	0.0111(4)	0.0118(4)	0.0121(3)	0.0114(4)
	$b22$	0.0358(17)	0.0347(9)	0.0301(11)	0.0327(13)	0.0341(10)	0.0335(13)
	$b33$	0.0109(6)	0.0106(3)	0.0109(4)	0.0114(5)	0.0118(4)	0.0116(4)
	$b12$	0.0008(9)	0.0010(5)	0.0013(6)	0.0016(10)	−0.0003(12)	−0.0036(16)
	$b13$	0.0013(5)	0.0004(3)	0.0003(3)	0.0004(4)	−0.0006(3)	0.0000(3)
	$b23$	−0.0021(10)	−0.0025(5)	−0.0012(6)	−0.0016(8)	−0.0018(10)	−0.0011(27)
O1	x	0.3272(23)	0.3315(13)	0.3273(16)	0.3268(18)	0.3275(13)	0.3328(15)
	y	0	0	0	0	0	0
	z	3/4	3/4	3/4	3/4	3/4	3/4
	$b11$	0.0248(34)	0.0287(20)	0.0297(26)	0.0317(31)	0.344(24)	0.0352(23)
	$b22$	0.1046(144)	0.0931(71)	0.0964(91)	0.0987(101)	0.1023(74)	0.1057(74)
	$b33$	0.0111(25)	0.0112(13)	0.0117(17)	0.0112(19)	0.0131(15)	0.0123(13)
	$b23$	0.0083(49)	0.0070(26)	0.0079(36)	0.0089(51)	0.0068(66)	−0.0048(143)
O2	x	0	0	0	0	0	0
	y	0.5774(65)	0.5714(36)	0.5572(56)	0.5401(70)	0.5252(94)	0.5163(307)
	z	1/2	1/2	1/2	1/2	1/2	1/2
	$b11$	0.0084(19)	0.0107(12)	0.0116(15)	0.0133(18)	0.0127(13)	0.0138(14)
	$b22$	0.1338(212)	0.1390(116)	0.1496(158)	0.1452(159)	0.1699(138)	0.1403(161)
	$b33$	0.0328(45)	0.0356(25)	0.0356(33)	0.0387(39)	0.0365(25)	0.0395(26)
	$b13$	−0.0054(28)	−0.0004(17)	−0.0004(22)	−0.0033(27)	0.0082(18)	0.0104(19)
O3	x	0.2503(23)	0.2535(11)	0.2533(16)	0.2554(20)	0.2487(41)	0.2548(125)
	y	0.3182(36)	0.3176(15)	0.3030(21)	0.2853(29)	0.2655(37)	0.2530(116)
	z	0.5301(20)	0.5292(10)	0.5216(16)	0.5130(26)	0.5049(37)	0.4956(47)
	$b11$	0.0345(30)	0.0366(17)	0.0364(20)	0.0380(24)	0.0400(18)	0.0357(26)
	$b22$	0.0847(92)	0.0630(40)	0.0591(51)	0.0667(55)	0.0762(43)	0.0649(40)
	$b33$	0.0256(38)	0.0262(20)	0.0312(26)	0.0359(29)	0.0385(20)	0.0400(20)
	$b12$	0.0273(51)	0.0254(24)	0.0208(29)	0.0232(34)	0.0263(27)	0.0228(27)
	$b13$	0.0007(32)	−0.0045(16)	−0.0041(22)	−0.0023(26)	−0.0069(20)	−0.0051(20)
	$b23$	0.0057(50)	0.0091(24)	0.0102(33)	0.0139(46)	0.0132(36)	0.0173(30)

[a] Specimen A # 3. [b] Specimen A # 13. Entries for 693 and 733 K are values obtained by assuming orthorhombic cells.

Structural change of orthorhombic-

Table 3. Atomic parameters at 693 model.

	693 K	
	Si	O1
x	1/3	1/3
y	2/3	2/3
z	0.4379(4)	1/4
$b11$	0.0473(16)	0.1433(88)
$b22$	0.0473	0.1433
$b33$	0.0116(5)	0.0118(17)
$b12$	0.0237	0.0717
$b13$	0.0	0.0
$b23$	0.0	0.0

E.s.d.'s are in parentheses.

Table 4. Final R-values, R_w and R_s and 733 K.

	443 [a]	493 [a]	573 [a]
R_w	0.141	0.076	0.100
R	0.145	0.092	0.102
S	3.337	1.760	2.349
N°	322	322	322
p°	30	30	30

[a] Number of reflections.
[b] Number of parameters varied.
[c] Specimen A # 3.
[d] Specimen A # 13.
Values for hexagonal refinements are

least-squares program, which i
1962), was used. Weighting sch
atomic scattering factors were
in the *International Tables for*

The refinement, assuming c
converged at a structure withou
ormal Gibbs structure (Gibbs,
hand, in the refinement for th
hexagonal positions are larger t
parameters, and also larger th
have observed no significant c
the intensity distribution. The
refined to acceptably low R-va
733 K data, respectively (Table

$b33$	0.0111(25)	0.0112(13)	0.0117(17)	0.0112(19)																			
$b23$	0.0083(49)	0.0070(26)	0.0079(36)	0.0089(51)																			
O2																							
x	0	0	0	0	0	0	0	0	0	0	0	0	0	0	0	0	0	0	0	0	0	0	0
y	0.5774(65)	0.5714(36)	0.5572(56)	0.5401(70)	0.5252(94)	0.5163(307)																	
z	1/2	1/2	1/2	1/2	1/2	1/2																	
$b11$	0.0084(19)	0.0107(12)	0.0116(15)	0.0133(18)	0.0127(13)	0.0138(14)																	
$b22$	0.1338(212)	0.1390(116)	0.1496(158)	0.1452(159)	0.1699(138)	0.1403(161)																	
$b33$	0.0328(45)	0.0356(25)	0.0356(33)	0.0387(39)	0.0365(25)	0.0395(26)																	
$b13$	−0.0054(28)	−0.0004(17)	−0.0004(22)	−0.0033(27)	0.0082(18)	0.0104(19)																	
O3																							
x	0.2503(23)	0.2535(11)	0.2533(16)	0.2554(20)	0.2487(41)	0.2548(125)																	
y	0.3182(36)	0.3176(15)	0.3030(21)	0.2853(29)	0.2655(37)	0.2530(116)																	
z	0.5301(20)	0.5292(10)	0.5216(16)	0.5130(26)	0.5049(37)	0.4956(47)																	
$b11$	0.0345(30)	0.0366(17)	0.0364(20)	0.0380(24)	0.0400(18)	0.0357(26)																	
$b22$	0.0847(92)	0.0630(40)	0.0591(51)	0.0667(55)	0.0762(43)	0.0649(40)																	
$b33$	0.0256(38)	0.0262(20)	0.0312(26)	0.0359(29)	0.0385(20)	0.0400(20)																	
$b12$	0.0273(51)	0.0254(24)	0.0208(29)	0.0232(34)	0.0263(27)	0.0228(27)																	
$b13$	0.0007(32)	−0.0045(16)	−0.0041(22)	−0.0023(26)	−0.0069(20)	−0.0051(20)																	
$b23$	0.0057(50)	0.0091(24)	0.0102(33)	0.0139(46)	0.0132(36)	0.0173(30)																	

[a] Specimen A # 3. [b] Specimen A # 13. Entries for 693 and 733 K are values obtained by assuming orthorhombic cells.

Table 3. Atomic parameters at 693 and 733 K: Refinements based on hexagonal Gibbs model.

	693 K			733 K		
	Si	O1	O2	Si	O1	O2
x	1/3	1/3	0	1/3	1/3	0
y	2/3	2/3	1/2	2/3	2/3	1/2
z	0.4379(4)	1/4	0	0.4378(4)	1/4	0
$b11$	0.0473(16)	0.1433(88)	0.0577(49)	0.0472(16)	0.1376(87)	0.0576(55)
$b22$	0.0473	0.1433	0.1453(67)	0.0472	0.1376	0.1487(72)
$b33$	0.0116(5)	0.0118(17)	0.0411(19)	0.0116(5)	0.0124(19)	0.0404(19)
$b12$	0.0237	0.0717	0.0289	0.0236	0.0688	0.0289
$b13$	0.0	0.0	−0.0267(33)	0.0	0.0	−0.0252(34)
$b23$	0.0	0.0	−0.0134	0.0	0.0	−0.0126

E.s.d.'s are in parentheses.

Table 4. Final R-values, R_w and R, and "goodness of fit", S, at 443, 493, 573, 653, 693 and 733 K.

	443[a]	493[a]	573[a]	653[a]	693[a]	733[b]
R_w	0.141	0.076	0.100	0.118	0.077(0.069)	0.052(0.055)
R	0.145	0.092	0.102	0.118	0.104(0.084)	0.066(0.071)
S	3.337	1.760	2.349	2.647	1.679(1.633)	1.414(1.463)
N[c]	322	322	322	322	322(124)	176(82)
p[d]	30	30	30	30	30(11)	30(11)

[a] Number of reflections.
[b] Number of parameters varied.
[c] Specimen A # 3.
[d] Specimen A # 13.
Values for hexagonal refinements are in parentheses.

least-squares program, which is the 1977 version of *ORFLS* (Busing et al. 1962), was used. Weighting schemes were based on $w = 1/\sigma^2(F)$. Spherical atomic scattering factors were taken from the tables of Cromer and Waber in the *International Tables for X-ray Crystallography*, vol. IV (1974).

The refinement, assuming orthorhombic symmetry, for the 733 K data converged at a structure without any significant departure from the hexagonal Gibbs structure (Gibbs, 1927) of $P6_3/mmc$ (Table 3). On the other hand, in the refinement for the 693 K data, the displacements from the hexagonal positions are larger than the corresponding one-sigmas for some parameters, and also larger than those at 733 K. At 693 K, however, we have observed no significant departure from the hexagonal symmetry in the intensity distribution. The Gibbs hexagonal model was alternatively refined to acceptably low R-values of 0.069 and 0.055 for the 693 and the 733 K data, respectively (Table 4): the positional and even the temperature

parameters are essentially the same for the two refinements (Table 3). Therefore the structure can be reasonably assumed as hexagonal at 693 K, and we take the advantages of the small number of the parameters and low correlations between the parameters in $P6_3/mmc$. Table 5 shows selected interatomic distances and angles.

Discussion

The present second-order refinements based on the Dollase model resulted in rather high R-values: the final weighted R-values, R_w, are in the range from 0.069 to 0.141 for the five data sets (Table 4). The reported R-values for Dollase's refinement of the Steinbach tridymite is also as high as 0.086. In the present refinements, the calculated structure factors for 60 l with odd l are significantly smaller than the observed ones, as in the case for the Steinbach tridymite (Dollase, 1967). The high R-values and the large systematic discrepancies between the observed and the calculated structure factors, common to the two independent studies, are indicative of shortcoming of the structural model adopted here and previously. The present refinements are, therefore, obviously insufficient to express accurate atomic density distribution, but may be still useful to estimate the mean positions and dispersions of the density distribution. (Least-squares calculations based on higher-order thermal tensors were attempted to improve the agreements between the observed and the calculated structure factors: the result will appear elsewhere in this journal.)

Table 6 shows the m.s.d.'s, $\langle u^2 \rangle$, in the principal axes of the thermal ellipsoids. The thermal ellipsoids of O are oriented so that the axes of the smallest m.s.d.'s are nearly parallel to the lines joining two Si atoms bonded to the O atoms. In the following discussion, we express the smallest, the intermediate and the largest m.s.d.'s along the principal axes of the thermal ellipsoids, with symbols S, I and L, respectively. The thermal ellipsoids of O1, at the five temperatures in the $O-I$ range, are well approximated by oblate-spheroidal shapes, while those for O2 and O3 are no longer circular, but elliptical in the planes perpendicular to the S directions.

In Figure 1, the m.s.d.'s of Si and O along the principal axes of the thermal ellipsoids are shown as functions of temperature. The m.s.d.'s of O1 are separated into two groups on the basis of their magnitudes, $(O1)_{L,I}$ and $(O1)_S$, while those of O2 and O3 into three groups, $(O2,O3)L$, $(O2,O3)_I$ and $(O2,O3)_S$. The m.s.d.'s with commas, (,), indicate to be averaged over atoms or directions: for example; $(O1)_{L,I}$ is the average over the m.s.d.'s along the L and I directions for O1, and $(O2,O3)_L$ over the L directions for O2 and O3, and so on. The m.s.d.'s for Si, in Figure 1, are averaged over the three directions. Only the overall averaged values for O and Si are shown for M (Bauer, 1977), because the m.s.d.'s of the two kinds of atoms are quite small in comparison with those in the higher-temperature forms.

Table 5. Atomic distances (Å) and angles (°) at 443, 493, 573, 653, 693 and 733 K. Uncorrected for disorder and thermal vibrations.

	443 K [a]	493 K [a]	573 K [a]	653 K [a]	693 K [b]	733 K [c]
Si−O1′	1.563(4)	1.562(3)	1.559(4)	1.558(4)	1.553(3)	1.555(5)
−O2	1.562(5)	1.562(3)	1.564(4)	1.563(4)	1.545(2)	1.546(3)
−O3	1.561(19)	1.565(9)	1.549(13)	1.544(17)	1.545	1.546
−O3′	1.534(19)	1.547(9)	1.551(12)	1.538(16)	1.545	1.546
Average	1.555	1.559	1.556	1.551	1.547	1.548
O1′−O2	2.575(13)	2.554(7)	2.571(9)	2.567(10)	2.529(2)	2.530(4)
−O3	2.562(18)	2.579(9)	2.547(14)	2.530(20)	2.529	2.530
−O3′	2.497(18)	2.510(9)	2.508(13)	2.508(20)	2.529	2.530
O2−O3	2.553(26)	2.571(13)	2.569(20)	[illegible]		

ame for the two refinements (Table 3). asonably assumed as hexagonal at 693 K, small number of the parameters and low ters in $P6_3/mmc$. Table 5 shows selected

nents based on the Dollase model resulted l weighted R-values, R_w, are in the range lata sets (Table 4). The reported R-values einbach tridymite is also as high as 0.086. lculated structure factors for $60\,l$ with odd he observed ones, as in the case for the 967). The high R-values and the large the observed and the calculated structure independent studies, are indicative of nodel adopted here and previously. The re, obviously insufficient to express accu-, but may be still useful to estimate the of the density distribution. (Least-squares rder thermal tensors were attempted to the observed and the calculated structure ewhere in this journal.)

$u^2\rangle$, in the principal axes of the thermal of O are oriented so that the axes of the el to the lines joining two Si atoms bonded g discussion, we express the smallest, the l.'s along the principal axes of the thermal L, respectively. The thermal ellipsoids of he $O-I$ range, are well approximated by hose for O2 and O3 are no longer circular, ndicular to the S directions.

Si and O along the principal axes of the functions of temperature. The m.s.d.'s of s on the basis of their magnitudes, $(O1)_{L,I}$ O3 into three groups, $(O2,O3)L$, $(O2,O3)_I$ commas, (,), indicate to be averaged over ; $(O1)_{L,I}$ is the average over the m.s.d.'s 1, and $(O2,O3)_L$ over the L directions for d.'s for Si, in Figure 1, are averaged over verall averaged values for O and Si are use the m.s.d.'s of the two kinds of atoms th those in the higher-temperature forms.

Table 5. Atomic distances (Å) and angles (°) at 443, 493, 573, 653, 693 and 733 K. Uncorrected for disorder and thermal vibrations.

	443 K [a]	493 K [a]	573 K [a]	653 K [a]	693 K [b]	733 K [c]
Si−O1′	1.563(4)	1.562(3)	1.559(4)	1.558(4)	1.553(3)	1.555(5)
−O2	1.562(5)	1.562(3)	1.564(4)	1.563(4)	1.545(2)	1.546(3)
−O3	1.561(19)	1.565(9)	1.549(13)	1.544(17)	1.545	1.546
−O3′	1.534(19)	1.547(9)	1.551(12)	1.538(16)	1.545	1.546
Average	1.555	1.559	1.556	1.551	1.547	1.548
O1′−O2	2.575(13)	2.554(7)	2.571(9)	2.567(10)	2.529(2)	2.530(4)
−O3	2.562(18)	2.579(9)	2.547(14)	2.530(20)	2.529	2.530
−O3′	2.497(18)	2.510(9)	2.508(13)	2.508(20)	2.529	2.530
O2−O3	2.553(26)	2.571(13)	2.569(20)	2.578(25)	2.524(2)	2.526(4)
−O3′	2.502(25)	2.499(13)	2.498(20)	2.473(25)	2.524	2.526
O3−O3′	2.548(26)	2.558(11)	2.545(15)	2.534(21)	2.524	2.526
Average	2.540	2.545	2.540	2.532	2.527	2.528
Si−O1−Si	177.2(15)	179.7(9)	177.1(10)	177.1(12)	180.0	180.0
Si−O2−Si	170.4(24)	171.0(14)	171.9(20)	173.4(26)	180.0	180.0
Si−O3−Si	160.6(13)	160.6(6)	165.1(10)	170.0(15)	180.0	180.0
O1′−Si−O2	110.9(8)	109.7(5)	110.9(6)	110.7(7)	109.4(2)	109.4(2)
O3	110.1(8)	111.1(4)	110.1(6)	109.3(9)	109.4	109.4
O3′	107.4(8)	107.7(4)	107.5(6)	108.2(9)	109.4	109.4
O2−Si−O3	109.7(12)	110.6(6)	111.2(10)	112.2(13)	109.5(2)	109.6(2)
O2−Si−O3′	107.8(14)	107.0(7)	106.7(11)	105.8(14)	109.5	109.6
O3−Si−O3′	110.8(10)	110.6(5)	110.4(7)	110.6(10)	109.5	109.6

[a] From Table 2 (orthorhombic). [b] From Table 3 (hexagonal). [c] After Kihara (1978) (hexagonal). O1′ and O3′ are symmetrically related to O1 and O3, respectively, by a transformation, $(-x + 1/2, y + 1/2, -z + 1)$ in the orthorhombic cell.

Table 6. Mean-squares displacements along principal axes of Si and O thermal ellipsoids and their orientations: (A) 443, (B) 493, (C) 573, (D)653, (E) 693 and (F) 733 K. E.s.d.'s of m.s.d.'s are shown in parentheses.

Axes	Angles (°) from orthogonal coordinates, X(i)[a]							
	m.s.d.(Å^2)	X(1)	X(2)	X(3)	m.s.d.(Å^2)	X(1)	X(2)	X(3)
		(A)				(B)		
Si 1	0.027(2)	29	101	117	0.038(2)	9	85	62
2	0.047(3)	91	24	114	0.047(2)	82	26	115
3	0.038(2)	61	69	37	0.032(2)	118	65	39
O1 1(*I*)	0.096(14)	0	90	90	0.112(8)	0	90	90
2(*L*)	0.136(18)	90	10	80	0.121(9)	90	10	80
3(*S*)	0.035(9)	90	100	10	0.036(5)	90	100	10
O2 1(*S*)	0.028(8)	13	90	77	0.042(5)	1	90	89
2(*L*)	0.169(27)	90	0	90	0.177(15)	90	0	90
3(*I*)	0.116(15)	103	90	13	0.122(9)	91	90	1
O3 1(*L*)	0.183(12)	40	51	84	0.176(7)	30	60	93
2(*S*)	0.056(12)	127	40	104	0.035(6)	118	39	115
3(*I*)	0.088(13)	103	83	15	0.101(7)	100	67	25
		(C)				(D)		
Si 1	0.045(2)	25	65	90	0.048(2)	34	57	93
2	0.40(2)	107	50	135	0.043(2)	116	54	133
3	0.034(2)	108	51	45	0.036(2)	110	54	43
O1 1(*I*)	0.116(11)	0	90	90	0.123(13)	0	90	90
2(*L*)	0.127(12)	90	11	79	0.131(13)	90	11	79
3(*S*)	0.037(7)	90	101	11	0.035(7)	90	102	12
O2 1(*S*)	0.046(6)	1	90	89	0.050(8)	8	90	82
2(*L*)	0.192(21)	90	0	90	0.187(21)	90	0	90
3(*I*)	0.122(12)	91	90	1	0.135(14)	98	90	8
O3 1(*L*)	0.166(8)	27	64	94	0.178(9)	33	59	81
2(*S*)	0.042(7)	116	35	112	0.045(8)	117	35	111
3(*I*)	0.117(9)	96	69	22	0.134(10)	108	77	23
		(E)				(F)		
Si 1	0.046(1)	0	90	90	0.046(1)	0	90	90
2	0.046	90	0	90	0.046	90	0	90
3	0.040(2)	90	90	0	0.040(2)	90	90	0
O1 1(*L*)	0.139(5)	0	90	90	0.134(5)	0	90	90
2(*L*)	0.139	90	0	90	0.134	90	0	90
3(*S*)	0.041(6)	90	90	0	0.043(7)	90	90	0
O2 1(*S*)	0.034(6)	24	90	66	0.036(6)	24	90	66
2(*L*)	0.169(10)	90	0	90	0.174(10)	90	0	90
3(*I*)	0.164(7)	114	90	24	0.160(7)	114	90	24

[a] For example, see Lipson and Cochran (1966).
L, *I* and *S* in parentheses indicate principal axes corresponding to the largest, the intermediate and the smallest values of m.s.d.'s, respectively.

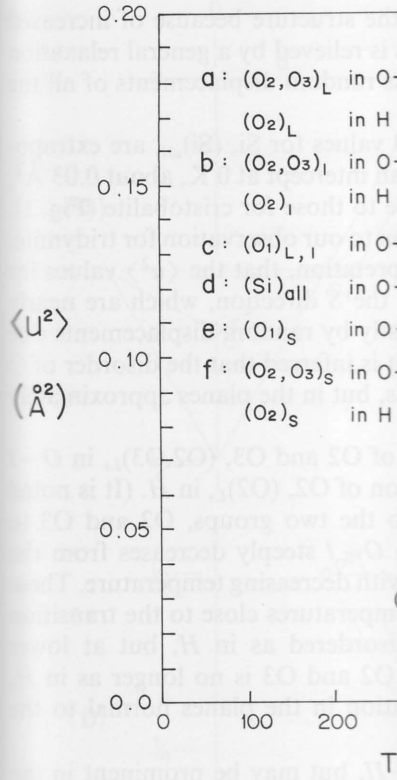

Fig. 1. Mean-square displacements for S
Atoms written with parentheses, for exa
mean-square displacements. For the det
(*M*) and orthorhombic-*II* (*O*−*II*) are r
The broken line indicates $\langle u^2 \rangle$ vs. *T* rela
1973).

The m.s.d.'s of O in *O*−*II* are sep
thermal ellipsoids for O are well ap
with a few exceptional cases.

It may be noted that $(O1)_S$ in
in *H* are all nearly equal to $(Si)_{all}$,
much larger than $(Si)_{all}$. The larg
positional disorder of O.

According to Leadbetter et al
in the structure of high cristobalit
of positions. Leadbetter et al. hav
linearly extrapolated it to an in
observation for high cristobalite

rincipal axes of Si and O thermal ellipsoids
73, (D)653, (E) 693 and (F) 733 K. E.s.d.'s

linates, X(i)[a]

3)	m.s.d.(Å^2)	X(1)	X(2)	X(3)
		(B)		
	0.038(2)	9	85	62
	0.047(2)	82	26	115
	0.032(2)	118	65	39
	0.112(8)	0	90	90
	0.121(9)	90	10	80
	0.036(5)	90	100	10
	0.042(5)	1	90	89
	0.177(15)	90	0	90
	0.122(9)	91	90	1
	0.176(7)	30	60	93
	0.035(6)	118	39	115
	0.101(7)	100	67	25
		(D)		
	0.048(2)	34	57	93
	0.043(2)	116	54	133
	0.036(2)	110	54	43
	0.123(13)	0	90	90
	0.131(13)	90	11	79
	0.035(7)	90	102	12
	0.050(8)	8	90	82
	0.187(21)	90	0	90
	0.135(14)	98	90	8
	0.178(9)	33	59	81
	0.045(8)	117	35	111
	0.134(10)	108	77	23
		(F)		
	0.046(1)	0	90	90
	0.046	90	0	90
	0.040(2)	90	90	0
	0.134(5)	0	90	90
	0.134	90	0	90
	0.043(7)	90	90	0
	0.036(6)	24	90	66
	0.174(10)	90	0	90
	0.160(7)	114	90	24

6).
axes corresponding to the largest, the
, respectively.

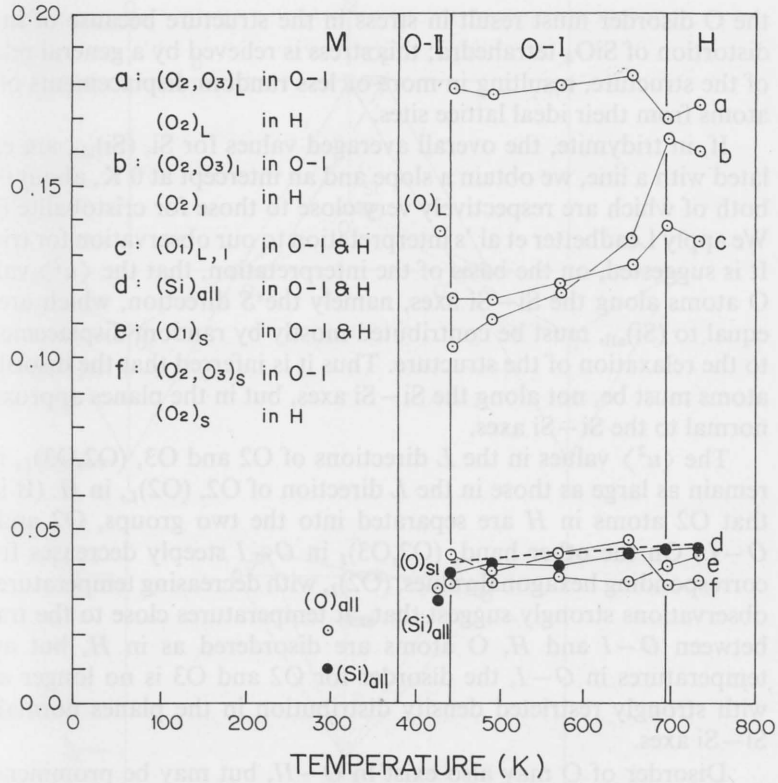

Fig. 1. Mean-square displacements for Si and O in tridymite as functions of temperature. Atoms written with parentheses, for example $(O2,O3)_L$, $(O1)_{L,I}$ and so on, express their mean-square displacements. For the details of the notation, see text. Data for monoclinic (*M*) and orthorhombic-*II* (*O*−*II*) are respectively from Baur (1977) and Kihara (1977). The broken line indicates $\langle u^2 \rangle$ vs. *T* relation for Si in high cristobalite (Leadbetter et al., 1973).

The m.s.d.'s of O in *O*−*II* are separated into $(O)_L$ and $(O)_{S,I}$, because the thermal ellipsoids for O are well approximated to prolate-spheroidal shapes with a few exceptional cases.

It may be noted that $(O1)_S$ in *O*−*I* and *H*, $(O2,O3)_S$ in *O*−*I* and $(O2)_S$ in *H* are all nearly equal to $(Si)_{all}$, but $(O2,O3)_L$, $(O2,O3)_I$ and $(O1)_{L,I}$ are much larger than $(Si)_{all}$. The large $\langle u^2 \rangle$ values in *O*−*I* strongly suggest positional disorder of O.

According to Leadbetter et al. (1973) and Peacor (1973), the O atoms in the structure of high cristobalite are positionally disordered over six sets of positions. Leadbetter et al. have plotted $\langle u^2 \rangle$ vs. *T* relation for Si and linearly extrapolated it to an intercept, 0.033 Å^2, at 0 K (Fig. 1). This observation for high cristobalite is interpreted by themselves as follows:

the O disorder must result in stress in the structure because of increased distortion of SiO_4 tetrahedra; this stress is relieved by a general relaxation of the structure, resulting in more or less random displacements of all the atoms from their ideal lattice sites.

If, in tridymite, the overall averaged values for Si, $(Si)_{all}$, are extrapolated with a line, we obtain a slope and an intercept at 0 K, about 0.03 Å^2, both of which are respectively very close to those for cristobalite (Fig. 1). We apply Leadbetter et al.'s interpretation to our observation for tridymite. It is suggested, on the basis of the interpretation, that the $\langle u^2 \rangle$ values for O atoms along the Si–Si axes, namely the S direction, which are nearly equal to $(Si)_{all}$, must be contributed mostly by random displacements due to the relaxation of the structure. Thus it is inferred that the disorder of O atoms must be, not along the Si–Si axes, but in the planes approximately normal to the Si–Si axes.

The $\langle u^2 \rangle$ values in the L directions of O2 and O3, $(O2,O3)_L$, in $O-I$ remain as large as those in the L direction of O2, $(O2)_L$, in H. (It is noted that O2 atoms in H are separated into the two groups, O2 and O3 in $O-I$.) On the other hand, $(O2,O3)_I$ in $O-I$ steeply decreases from the corresponding hexagonal values, $(O2)_I$, with decreasing temperature. These observations strongly suggest that, at temperatures close to the transition between $O-I$ and H, O atoms are disordered as in H, but at lower temperatures in $O-I$, the disorder for O2 and O3 is no longer as in H, with strongly restricted density distribution in the planes normal to the Si–Si axes.

Disorder of O may also exist in $O-II$, but may be prominent in the single directions perpendicular to the Si–Si axes, since only $(O)_L$ is still as large as those in $O-I$ and H. We have only the room temperature values of the m.s.d.'s for Si and O in M (Kato and Nukui, 1976; Baur, 1977), which are too small to assume disorder for the atoms.

Figure 2 shows the mean positions of Si, O1, O2 and O3 in the orthorhombic refinements, at the five temperatures. The thermal expansion of the cell is neglected in Figure 2. The structural change of $O-I$ is brought about by pair-wise rotations of any two tetrahedra joined by O1, around two-fold axes parallel to **a** and passing O1. The x-coordinates of all the atoms are therefore kept constant during the rotation. Thus with increasing temperature the pair-wise rotations of the tetrahedra around **a** brings the atomic mean positions directly to those in $P6_3/mmc$. To obtain the positions in $P6_322$, the possibility of which was suggested by Kihara (1978), another rotation around **c** is inevitable, in addition to that around **a**. Since we have observed no rotations around **c** the possibility of $P6_322$ is disregarded.

Each of the successive structure transitions in tridymite, except for that between M and $O-II$, thus occurs between the structures including disorder of O. Tridymite is a unique mineral, not only for showing successive transitions, but also for showing the 'disorder to disorder' tran-

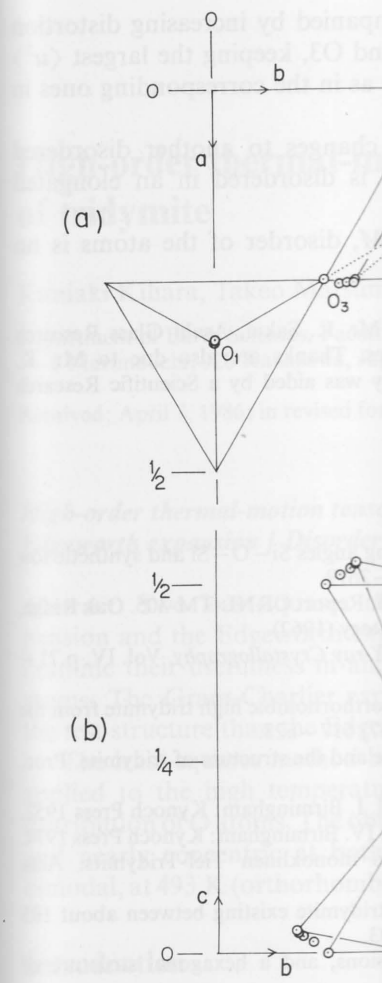

Fig. 2. Schematic views of structural ch
(b) Projection on to (100). Tridymite
443 K. Mean positions for O are show
H to those at 443 K. Thermal expansi

sitions. The structural changes
temperature lowers.

(1) After the transition to O
pair-wise rotatory changes in o
O1 progressively occur around t
with decreasing temperature. (T
or vice versa shows no notable
data obtained by Thompson an

ss in the structure because of increased
stress is relieved by a general relaxation
or less random displacements of all the

raged values for Si, $(Si)_{all}$, are extrapo-
and an intercept at 0 K, about 0.03 Å^2,
/ close to those for cristobalite (Fig. 1).
etation to our observation for tridymite.
interpretation, that the $\langle u^2 \rangle$ values for
mely the S direction, which are nearly
d mostly by random displacements due
Thus it is inferred that the disorder of O
Si axes, but in the planes approximately

tions of O2 and O3, $(O2,O3)_L$, in $O-I$
irection of O2, $(O2)_L$, in H. (It is noted
d into the two groups, O2 and O3 in
$3)_I$ in $O-I$ steeply decreases from the
$2)_I$, with decreasing temperature. These
at temperatures close to the transition
are disordered as in H, but at lower
r for O2 and O3 is no longer as in H,
stribution in the planes normal to the

n $O-II$, but may be prominent in the
he Si – Si axes, since only $(O)_L$ is still as
have only the room temperature values
(Kato and Nukui, 1976; Baur, 1977),
rder for the atoms.
sitions of Si, O1, O2 and O3 in the
ve temperatures. The thermal expansion
The structural change of $O-I$ is brought
y two tetrahedra joined by O1, around
ssing O1. The x-coordinates of all the
uring the rotation. Thus with increasing
s of the tetrahedra around **a** brings the
ose in $P6_3/mmc$. To obtain the positions
vas suggested by Kihara (1978), another
ddition to that around **a**. Since we have
possibility of $P6_322$ is disregarded.
re transitions in tridymite, except for
occurs between the structures including
nique mineral, not only for showing
showing the 'disorder to disorder' tran-

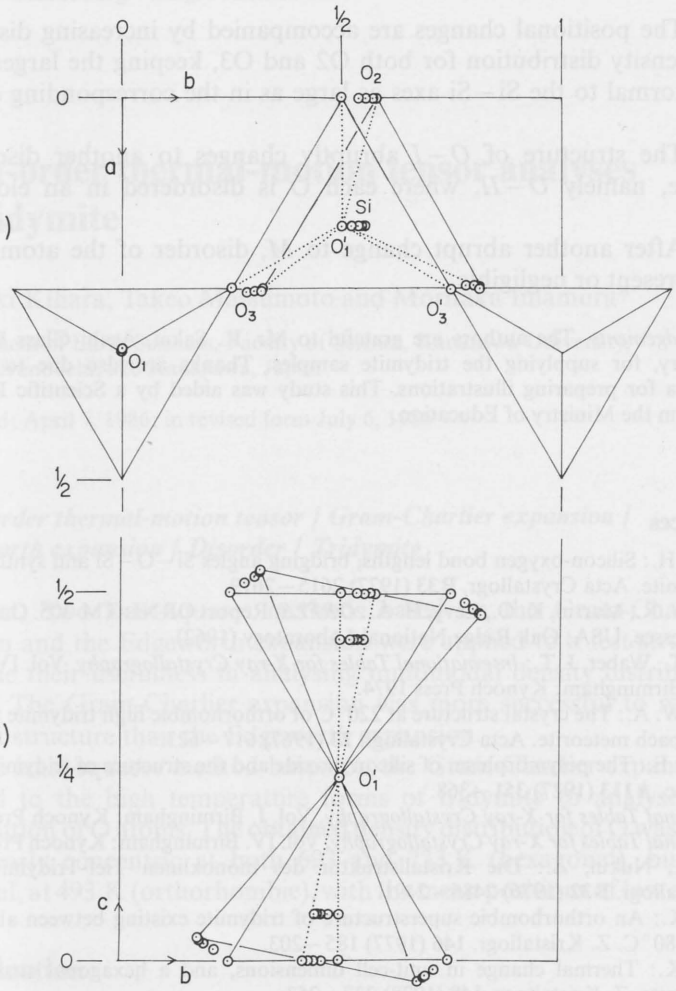

Fig. 2. Schematic views of structural change in tridymite $O-I$. (a) Projection on to (001). (b) Projection on to (100). Tridymite frameworks are shown only for cases of H and 443 K. Mean positions for O are shown with small open circles on paths from those of H to those at 443 K. Thermal expansions are neglected.

sitions. The structural changes are briefly summarized as follows, when temperature lowers.

(1) After the transition to $O-I$, where O atoms are still disordered, the pair-wise rotatory changes in orientation of any two tetrahedra joined by O1 progressively occur around two-fold axes, parallel to **a** and passing O1, with decreasing temperature. (The continuous transition from H to $O-I$ or vice versa shows no notable heat capasity effect, according to the DSC data obtained by Thompson and Wennemer, 1979.)

(2) The positional changes are accompanied by increasing distortion of the density distribution for both O2 and O3, keeping the largest $\langle u^2 \rangle$ values normal to the Si – Si axes as large as in the corresponding ones in *H*.

(3) The structure of *O – I* abruptly changes to another disordered structure, namely *O – II*, where each O is disordered in an elongated volume.

(4) After another abrupt change to *M*, disorder of the atoms is no longer present or negligible.

Acknowledgements. The authors are grateful to Mr. K. Sakai, Asahi Glass Research Laboratory, for supplying the tridymite samples. Thanks are also due to Mr. K. Nakamura for preparing illustrations. This study was aided by a Scientific Research Grant from the Ministry of Education.

References

Baur, W. H.: Silicon-oxygen bond lengths, bridging angles Si – O – Si and synthetic low tridymite. Acta Crystallogr. **B33** (1977) 2615 – 2619.

Busing, W. R., Martin, K. O., Levy, H. A.: *ORFLS*. Report ORNL-TM-305. Oak Ridge, Tennessee, USA: Oak Ridge National Laboratory (1962).

Cromer, T., Waber, J. T.: *International Tables for X-ray Crystallography*, Vol. IV, p.71 – 147. Birmingham: Kynoch Press 1974.

Dollase, W. A.: The crystal structure at 220 °C of orthorhombic high tridymite from the Steinbach meteorite. Acta Crystallogr. **23** (1967) 617 – 623.

Gibbs, R. E.: The polymorphism of silicon dioxide and the structure of tridymite. Proc. R. Soc. **A113** (1927) 351 – 368.

International Tables for X-ray Crystallography, Vol. I. Birmingham: Kynoch Press 1952.

International Tables for X-ray Crystallography, Vol. IV. Birmingham: Kynoch Press 1974.

Kato, K., Nukui, A.: Die Kristallstruktur des monoklinen Tief-Tridymits. Acta Crystallogr. **B32** (1976) 2486 – 2491.

Kihara, K.: An orthorhombic superstructure of tridymite existing between about 105 and 180 °C. Z. Kristallogr. **146** (1977) 185 – 203.

Kihara, K.: Thermal change in unit-cell dimensions, and a hexagonal structure of tridymite. Z. Kristallogr. **148** (1978) 237 – 253.

Kihara, K.: On the split-atom model for hexagonal tridymite. Z. Kristallogr. **152** (1980) 95 – 101.

Leadbetter, A. J., Smith, T. W., Wright, A. F.: Structure of high cristobalite. Nature (London) Phys. Sci. **244** (1973) 125 – 126.

Lipson, H., Cochran, W.: *The determination of crystal structures*. The crystalline state. Vol. III, (Sir L. Bragg, ed.). London: G. Bell and Sons Ltd. 1966.

Nukui, A., Nakazawa, H., Akao, M.: Thermal changes in monoclinic tridymite. Am. Mineral. **63** (1978) 1252 – 1259.

Peacor, D. R.: High temperature single-crystal study of the cristobalite inversion. Z. Kristallogr. **138** (1973) 274 – 298.

Schneider, H., Flörke, O. W., Majdic, A.: Thermal expansion of tridymite. Proc. Br. Ceram. Soc. No. **28** (1977) 267 – 279.

Thompson, A. B., Wennemer, M.: Heat capacities and inversions in tridymite, cristobalite, and tridymite-cristobalite mixed phases. Am. Mineral. **64** (1979) 1018 – 1026.

Zeitschrift für Kristallographie 177, 39-
© by R. Oldenbourg Verlag, München

High-order thermal-mo of tridymite

Kuniaki Kihara, Takeo Matsumo

Department of Earth Sciences, Faculty
1 – 1 Marunouchi, 920 Kanazawa, Jap

Received: April 7, 1986; in revised form

High-order thermal-motion tensor Edgeworth expansion | Disorder |

Abstract. Two least-squares me pansion and the Edgeworth exp examine their usefulness in anal atoms. The Gram-Charlier exp the test structure than the Edgew

The least-squares method ba applied to the high temperatur distribution of O atoms. The obta and nearly concentric at both bimodal, at 493 K (orthorhombic

Introduction

Structures of tridymite at six tem relationships among its four orthorhombic-*II* (*O – II*), orthor discussed in terms of disorder of tetrahedra based on the second (Kihara et al., 1986).

The second-order least-squa (Kihara, 1978) and of the Dollas et al., 1986) showed unusually la O. The thermal ellipsoids of all

* *Present address:* Seien Joshi Gak Japan.